Lead Article

Acta Cryst. (1991). B47, 824–835

Protein Engineering of Rubisco*

BY CARL-IVAR BRÄNDÉN, YLVA LINDQVIST AND GUNTER SCHNEIDER

Department of Molecular Biology, University of Agricultural Sciences, Biomedical Center, Box 590, S-751 24 Uppsala, Sweden

(*Received* 14 *January* 1991; *accepted* 18 *June* 1991)

Abstract

Modification of the kinetic parameters of enzymes by protein engineering requires extensive knowledge of the structural details of the enzyme and its complexes with different reaction intermediate analogues. Such structural studies are described here for Rubisco, ribulose-1,5-bisphosphate carboxylase/oxygenase, which catalyzes the initial reactions of two important but competing physiological events in green plants; carbon dioxide fixation and photorespiration. Observed functional changes in mutants of Rubisco are correlated with structural details as well as with the defined conformational changes that occur during catalysis. A possible functional role of the small subunit of Rubisco is described based on a comparison of the active-site geometry of a bacterial L_2 molecule with that of higher plant L_8S_8 molecules. The ultimate aim of these studies is to engineer Rubisco mutants that are more efficient than the wild-type enzyme by decreasing the oxygenase/carboxylase ratio.

Introduction

Green plants use most of the chemical energy trapped by the light reactions of photosynthesis to drive the fixation of carbon dioxide. This is brought about through a series of cyclic reactions, commonly referred to as the reductive pentose phosphate pathway or Calvin cycle. It is the only known way by which carbon dioxide can be incorporated into the biosphere in significant amounts.

The initial step of the photosynthetic fixation of carbon dioxide, the carboxylation of ribulose-1,5-bisphosphate (RuBP), is catalyzed by the enzyme ribulose-1,5-bisphosphate carboxylase/oxygenase (Rubisco). The reaction products are two molecules of 3-phosphoglycerate (PGA), which are partly recycled in the Calvin cycle to regenerate the carbon dioxide acceptor, RuBP, and partly converted to starch. This pathway is responsible for the annual net fixation of 10^{11} tons of CO_2 into the biosphere, a process upon which all agriculture ultimately depends. In C3 plants, the same enzyme also initiates a competing metabolic pathway, photorespiration. Here, the addition to RuBP of O_2 instead of CO_2 yields one molecule of PGA and one molecule of phosphoglycolate. The latter is metabolized in the glycolate pathway eventually producing CO_2 and energy in the form of heat. This pathway reduces the net efficiency of photosynthesis by up to 50%. Under most conditions photosynthetic efficiency and consequently crop yield is limited due to the oxygenase activity of this single enzyme. The genetic redesign of Rubisco with the aim of improving the carboxylation/oxygenation ratio and possibly increasing agricultural crop production has therefore attracted a lot of interest.

Two forms of Rubisco are found [for recent reviews see Andrews & Lorimer (1987) and Miziorko & Lorimer (1983)]. In higher plants, algae and most other photosynthetic organisms, the enzyme is a complex molecule consisting of eight large (L, M_r = 55 000) and eight small (S, M_r = 14 000) subunits, forming an L_8S_8 complex. In the photosynthetic bacterium *Rhodospirillum rubrum* on the other hand, the enzyme is a dimer of large subunits, L_2 (Tabita & McFadden, 1974). The L subunit carries the catalytic function. The overall amino-acid homology between the L subunits of L_2 and L_8S_8-type Rubisco is approximately 25%.

The gene for the L subunit of Rubisco from *Rh. rubrum* has been cloned and expressed in *E. coli* (Somerville & Somerville, 1984; Pierce & Gutteridge, 1985). The gene product was shown to be a fusion protein consisting of Rubisco and 24 additional amino acids from β-galactosidase at the N-terminus. The catalytic and kinetic properties of this fusion protein are indistinguishable from the wild-type enzyme. An expression system for an L_8S_8-type Rubisco, the enzyme from the cyanobacterium *Synechococcus* PCC6301, has been developed

* *Editorial note*: This invited paper is one of a series of comprehensive Lead Articles which the Editors invite from time to time on subjects considered to be timely for such treatment.

0108-7681/91/060824-16$03.00

(Kettleborough, Perry, Burton, Gutteridge, Keys & Philips, 1987). However, bacterial expression vectors containing the structural genes for the *L* and *S* subunits of higher plant Rubisco do not produce active enzyme (Gatenby, van der Vies & Rothstein, 1987), probably due to absence in *E. coli* of the chaperonin protein needed for assembly of L_8S_8-type Rubisco from higher plants (Barraclough & Ellis, 1980; Ellis & van der Vies, 1988).

Reaction mechanism of Rubisco

All Rubisco enzymes characterized so far require an activation process in order to become catalytically competent. Activation of the enzyme proceeds through the carbamylation of a lysine side chain by a CO_2 molecule. This activating CO_2 is distinct from the substrate CO_2 molecule. The carbamate is then stabilized by an Mg^{II} ion, yielding the active ternary complex enzyme–CO_2–Mg^{II} (Lorimer & Miziorko, 1980; Lorimer, 1981).

The series of chemical events for the carboxylation and the oxygenation reaction, as it is understood at present, is shown in Fig. 1, which is a more detailed form of the mechanism proposed already by Calvin (1956). The overall carboxylation reaction can be dissected into a series of partial reactions (Pierce, Lorimer & Reddy, 1986). These partial reactions have proven very useful in the analysis of site-directed mutants.

The reaction catalyzed by the activated enzyme starts with the enolization of RuBP, initiated by abstraction of the C(3) proton of the substrate. The enediol form then reacts with either CO_2 or O_2. It is

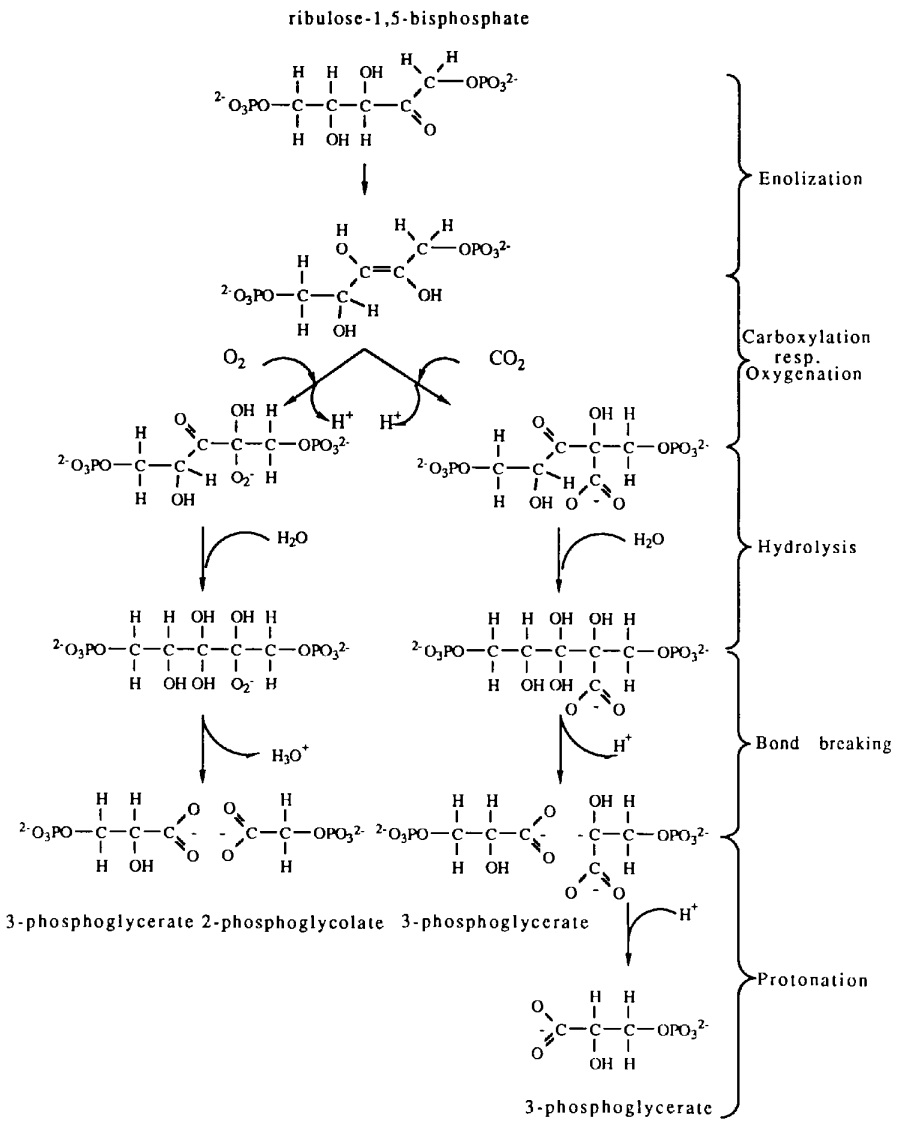

Fig. 1. Reaction mechanism of Rubisco.

at this stage during the catalytic cycle that the enzyme becomes dedicated to act either as a carboxylase or oxygenase. After this step, the enzyme is committed to either one of the reactions during one turnover. After carboxylation, the enzyme forms the reaction intermediate 2-carboxy-3-ketoarabinitol-1,5-bisphosphate (3-keto-CABP). Hydrolysis of 3-keto-CABP yields one molecule of PGA and a carbanion. Stereospecific protonation of the carbanion results in a second molecule of PGA. The reaction intermediate, 3-keto-CABP, is stable and can be isolated (Pierce *et al.*, 1986). This unique feature of the carboxylation reaction allows a thorough analysis of the catalytic deficiencies of site-directed mutants. When the reaction intermediate is given to activated wild-type enzyme as well as to some mutants with no overall catalytic activity, the reaction is completed and two molecules of phosphoglycerate are produced. Such inactive mutants obviously affect steps in the mechanism prior to carbon–carbon cleavage and hydrolysis. An analogue of the six-carbon intermediate, 2-carboxyarabinitol-1,5-bisphosphate (CABP) (Fig. 2), binds very tightly to the enzyme and acts as a potent inhibitor of enzyme activity.

The reaction mechanism for the oxygenation reaction is less well understood. This reaction is believed to proceed *via* the formation of a hydroxyperoxide intermediate that is subsequently cleaved yielding one molecule of phosphoglycerate and one molecule of phosphoglycolate. The latter enters the photorespiratory pathway ultimately producing CO_2.

Structure determination

Crystal structures are now available for the L_2- and L_8S_8-type of Rubisco both in the non-activated and activated forms of the enzyme (Schneider, Lindqvist, Brändén & Lorimer, 1986; Chapman, Suh, Cascio, Smith & Eisenberg, 1987; Chapman, Suh, Curmi, Cascio, Smith & Eisenberg, 1988; Andersson *et al.*, 1989; Knight, Andersson & Brändén, 1989, 1990; Lundqvist & Schneider, 1991; Schneider, Lindqvist & Lundqvist, 1990; Schneider, Knight, Andersson, Lindqvist, Lundqvist & Brändén, 1990).

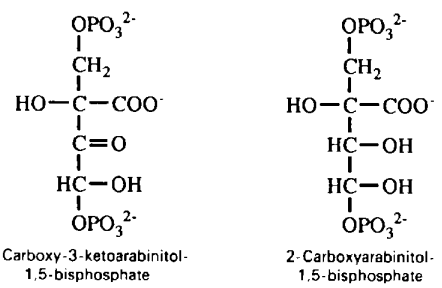

Fig. 2. The six-carbon reaction intermediate 2-carboxy-3-keto-arabinitol-1,5-bisphosphate (3-keto-CABP) and an analogue to this intermediate, 2-carboxyarabinitol-1,5-bisphosphate (CABP).

Rubisco from Rhodospirillum rubrum

Rubisco from *Rh. rubrum* has been crystallized in a number of different forms (Table 1). It is interesting to note that wild-type and recombinant Rubisco crystallize under similar conditions with identical cell dimensions (Choe, Jakob, Hahn & Pal, 1985). The monoclinic crystals of the non-activated enzyme diffract to 1·7 Å resolution and the structure of this enzyme species has been determined and refined at that resolution (Schneider, Lindqvist *et al.*, 1990). This structure was initially solved by a combination of MIR methods and phase refinement using twofold non-crystallographic symmetry at 2·9 Å resolution (Schneider, Lindqvist *et al.*, 1986). In the monoclinic form, the asymmetric unit contains the whole L_2 dimer. The two subunits are related by a local twofold symmetry axis. However, for some parts of the dimer, there are significant deviations from twofold symmetry, probably due to crystal packing.

The cyclic averaging of the symmetry-related electron densities was carried out using Bricogne's program package (Bricogne, 1976). The averaging procedure including all data to 2·9 Å resolution did not result in an interpretable electron density map. However, starting the averaging procedure at 5 Å resolution and extending the resolution in steps of one lattice point in all directions, using available MIR phase information, did improve the final electron density map so that most parts of the polypeptide chain could be traced. This initial model was subsequently extended and refined and the present crystallographic R value is 18% at 1·7 Å resolution (Schneider, Lindqvist *et al.*, 1990). Based on the three-dimensional structure of the non-activated enzyme, binary complexes of Rubisco with inhibitor and product as well as the activated ternary complex have been studied (Table 2).

Spinach Rubisco

Many different crystal forms of the L_8S_8 Rubisco molecule have been obtained, from both different laboratories and using enzyme derived from different species (Table 1). In no case has the activated and deactivated state of the enzyme crystallized in the same modification. David Eisenberg and his colleagues in Los Angeles have reported four crystal forms for the tobacco enzyme, one of which shows exact 422 symmetry in the L_8S_8 molecule. Our group in Uppsala has found three different crystal forms of the spinach enzyme, one of which is similar to the form reported for recombinant Rubisco from the cyanobacterium *Synechococcus* PCC6301. An orthorhombic crystal form with space group $C222_1$ has

Table 1. *Crystal forms of RuBP carboxylase*

Source	Species	Space group	Cell (Å)			No. of *L* subunits in asymmetric unit	Reference
			a	*b*	*c*		
Rh. rubrum	Activated	$P4_32_12$	82·2	82·2	290·9	2	(1)
Rh. rubrum	Activated	$P4_32_12$	83·0	83·0	290·0	2	(2)
Rh. rubrum	Non-activated	$P4_32_12$	82·4	82·4	324·0	2	(3)
Rh. rubrum	Non-activated	$P2_1$	65·5	70·6	104·1 $\beta = 92·1$	2	(4)
Rh. rubrum	Non-activated	$P2_12_12_1$	70·9	100·1	131·0	2	(4)
Spinach	Enzyme Mg^{II}–CO_2–CABP	$C222_1$	157·2	157·2	201·3	4	(5)
Spinach	Enzyme Mg^{II}–CO_2–CABP	$I422$	275	275	178	4	(6)
Spinach	Enzyme CABP	$P2_12_12_1$	184	119	218	4	(6)
Spinach	Activated	$C222_1$	158·6	158·6	203·4	4	(7)
Tobacco	Non-activated	$I4_132$	383	383	383	2	(8)
Tobacco	Non-activated	$P42_12$	230	230	315	6	(9)
Tobacco	Non-activated	$I422$	148·7	148·7	137·5	1	(10)
Tobacco	Enzyme–Mg^{II} CO_2–CABP	$P3_121$	204·6	204·6	117·4	4	(11)
Alcaligenes eutrophus	Enzyme–Mg^{II}–CO_2–CABP	$C222_1$	158·8	159·6	201·2	4	(12)
Chromatium vinosum	Activated	$I432$	245·9	245·9	245·9	2	(13)
Synechoccocus PC6301	Enzyme–Mg^{II}–CO_2–CABP	$P2_12_12_1$	111·9	199·7	223·9	8	(14)

References: (1) Janson *et al.* (1984); (2) Choe *et al.* (1985); (3) Schneider *et al.* (1984); (4) Schneider, Brändén & Lorimer (1986); (5) Andersson & Brändén (1984); (6) Andersson *et al.* (1983); (7) Barcena *et al.* (1983); (8) Baker *et al.* (1975); (9) Baker, Eisenberg & Eiserling (1977); (10) Baker, Suh & Eisenberg (1977); (11) Suh *et al.* (1987); (12) Pal *et al.* (1985); (13) Nakagawa *et al.* (1986); (14) Newman & Gutteridge (1990).

Table 2. *Crystal structures of RuBP carboxylase*

Source	Species	Resolution (Å)	Reference
Rh. rubrum	Native	1·7	(1)
Rh. rubrum	Enzyme–phosphoglycerate	2·9	(2)
Rh. rubrum	Enzyme–CABP	2·6	(3)
Rh. rubrum	Enzyme–CO_2–Mg^{2+}	2·3	(4)
Spinach	Enzyme–Mg^{2+}–CO_2–CABP	2·4	(5)
Tobacco	Native	2·8	(6)

References: (1) Schneider, Lindqvist *et al.* (1986, 1990); (2) Lundqvist & Schneider (1989*a*); (3) Lundqvist & Schneider (1989*b*); (4) Lundqvist & Schneider (1991); (5) Andersson *et al.* (1989); Knight *et al.* (1989, 1990); (6) Chapman *et al.* (1987, 1988).

been obtained for the spinach enzyme using very different crystallization conditions both by us and by Barcena, Pickersgill, Adams, Phillips & Whatley (1983) in Oxford. A similar crystal form has been reported by Saenger's group in Berlin (Pal, Jakob, Hahn, Bowien & Saenger, 1985) for Rubisco from the photosynthetic bacterium *Alcaligenes eutrophus*.

Since the Rubisco molecules in this orthorhombic crystal form exhibit pseudo-422 symmetry they pack in space group $C222_1$ in such a way as to produce a pseudo-tetragonal $F422$ unit cell. The pseudo tetragonality of these crystals is easily seen on the $hk0$ layer of the reciprocal lattice (Fig. 3). Interesting variations of the packing in this crystal form have been obtained by the three different groups. The crystals of Rubisco from *Alcaligenes eutrophus*, and frequently our crystals of the spinach enzyme, exhibit merohedral twinning, due to the similarity in packing the molecules along the *a* and *b* cell axes which is reflected in the similar lengths of these axes. The direction of the pseudo-fourfold axis is close to that of the *c* axis. We therefore tested all our spinach crystals prior to data collection and discarded those that were twinned. The crystals of the spinach enzyme obtained by the Oxford group exhibit disorder such that the origins of the molecules in every odd layer along *c* are shifted by around 4 Å in the **a** direction. In our spinach $C222_1$ crystals such disorder does not occur, in fact the crystals diffract beyond 1·5 Å, which is remarkable for a crystal with a protein mass of about 2 million dalton in the unit cell.

In these crystals half the L_8S_8 molecule is in the asymmetric unit. The pseudo-fourfold axis of the molecule is inclined 1° to the *c* axis of the crystal in the *a* direction. One of the molecular twofold axes is

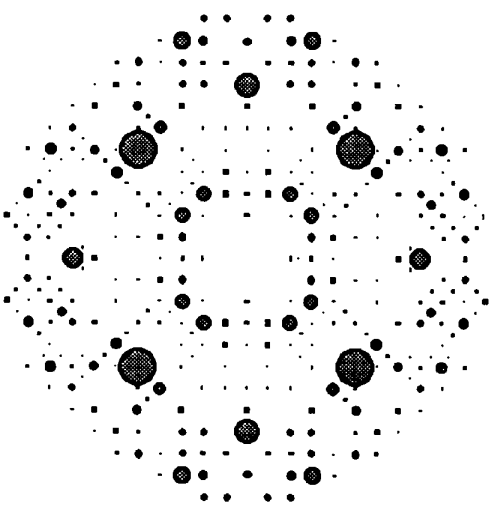

Fig. 3. $hk0$ layer of the reciprocal lattice of spinach Rubisco to 7 Å resolution. Space group $C222_1$ (Andersson & Brändén, 1984). The size of the circles is proportional to the intensity of the reflection.

therefore crystallographic, whereas the other is not. The deviations from strict 422 symmetry in the molecule are very small, in fact the model refined to an R value of 24% to 2·4 Å resolution using 422 symmetry constraints in the refinement procedure. All the high-resolution data, including native data as well as data for three heavy-atom derivatives, used for the determination of this spinach Rubisco structure were collected at synchrotron radiation sources, most of them in Daresbury using a wavelength of around 0·9 Å at the wiggler beam line.

The initial isomorphous electron density map, based on three heavy-atom derivatives, contained too large errors in the phase angles to be interpretable. In retrospect, this was probably due to the fact that almost all heavy-atom positions were by coincidence within two narrow sections of the molecule related by the crystallographic twofold axis along *b*. Not until we realized this and used all the heavy-atom positions of the molecule, not only those in the asymmetric unit, to define the exact direction of the fourfold axis did we obtain a sufficiently good definition of the local symmetry for the averaging and phase-refinement procedure (Bricogne, 1976) to produce an easily interpretable map.

Description of the structure

The L subunit

Despite the low amino-acid sequence identity, 28%, the overall structures of the large subunits of L_2-type Rubisco and L_8S_8-type Rubisco are very similar (Schneider, Knight *et al.*, 1990). The *L* subunit is built up of two domains (Fig. 4). The N-terminal domain, residues 1–150,* forms a central mixed five-stranded β sheet with two α helices on one side of the sheet. The larger C-terminal domain consists of amino acids 151–475. The central structural motif of this domain is the parallel β/α barrel which has been observed in a number of functionally non-related enzymes with completely different amino-acid sequences (Farber & Petsko, 1990). Eight parallel β strands form the core of a barrel, which is surrounded on the outside by eight α helices. The active site is located at the carboxyl side of the β strands, with several of the last residues in the β strands or the first residues in the loops between strands and helices being involved in catalysis.

The two domains of the subunit are clearly separated. The cleft formed between the two domains does not form the active site, but is utilized for subunit–subunit contacts. The amino-acid sequence at the domain–domain boundary (Gly150-Pro151) is conserved in all the Rubisco molecules whose amino-acid sequence is known. There are rather few interactions between the domains of the Rubisco subunit. One of the contact regions involves two anti-parallel strands in the loop between helix 6 and strand 7 of the β/α barrel. These two strands are almost parallel to the central β sheet of the N-terminal domain and are close to strand 5 of this mixed β sheet.

The L_2 dimer has the shape of a distorted ellipsoid with dimensions 45 × 70 × 105 Å with tight interactions between the subunits (Fig. 5). The core of the molecule is made up of the C-terminal domains from both subunits. The contacts at the interface between these domains involve interactions of the loops between the carboxyl ends of the β strands and the α helices from the β/α barrels across the local twofold axis of the molecule and cover an interaction area of 820 Å^2 (Schneider, Lindqvist *et al.*, 1990).

A second interface area between the two subunits is found between the N-terminal domain from one subunit and the C-terminal domain from the second subunit. Again, loop regions from the β/α barrel are involved in the subunit–subunit interactions. Amino-acid residues from loops 1, 2 and 3 interact with residues from the N-terminal domain of the second subunit. Amino-acid residues from the N-terminal domain which participate in these dimer interactions are found in loops and at the N-terminal end of helix *B*. Residues at the subunit–subunit interface also include the sequence 58–65, a highly conserved peptide region in all the Rubisco molecules. Glu60, which is at the C-terminal end of helix *A*, is part of an intricate network of charges and hydrogen bonds, involving the conserved charged side chains of residues Glu60, Lys175, Lys177, Asp203 and Glu204. The enzyme is not able to form dimers when Lys175 is replaced by an aspartate side chain (Soper, Larimer, Mural, Lee & Hartman, 1989). The replacement of a positive charge by a negative charge close to the cluster of negative charges from Glu60, Asp203 and Glu204 disrupts the balance of charges at this interface region. In the mutant, the negative charges of Glu60 and Asp175 repel each other and prevent dimerization (Fig. 5).

The active site of Rubisco is, like in all known β/α barrel enzymes, located at the C-terminal end of the eight parallel β strands. As a consequence of the subunit–subunit arrangement in the dimer, the active site is located at the interface between the two subunits, in a cleft formed between the C-terminal domain of one subunit and the N-terminal domain of the second subunit (Fig. 5). Parts from the N-terminal domain partly cover the active site and form a 'lid' at the carboxyl end of the barrel. Two regions

* All sequence numbering is based on the amino-acid sequence of Rubisco from spinach but in some cases the *Rh. rubrum* sequence numbers are also given for clarity. In the case of the *L* subunits, the unified numbering system suggested by Schneider, Knight *et al.* (1990) is used.

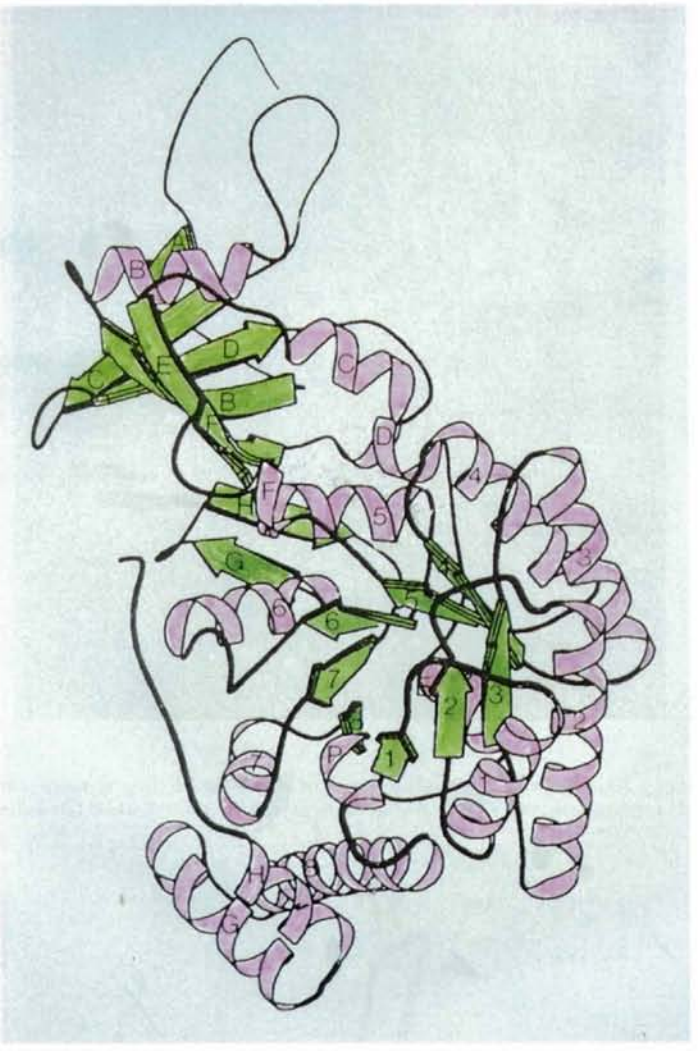

Fig. 4. Schematic representation of the structure of the *L* subunit of spinach Rubisco. β strands are depicted as arrows and α helices as cylinders (adapted from Knight *et al.*, 1990).

[*To face p.* 828

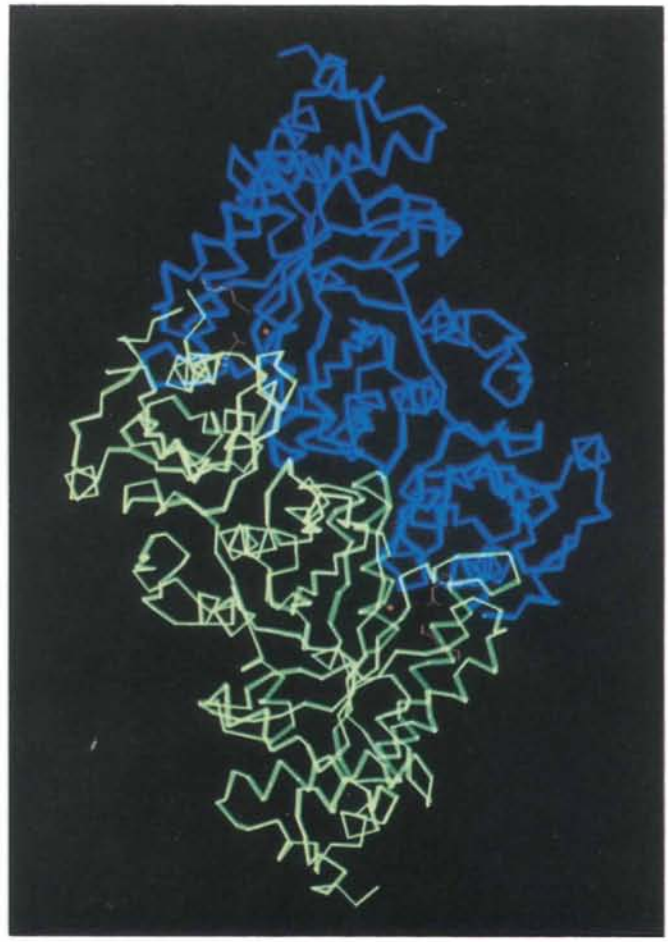

Fig. 5. Cα-tracing of the dimer of *Rh. rubrum* Rubisco. The positions of the active sites between subunits are indicated through the position of the Mg^{II} ions (red spheres) and two side chains in each active site, Lys177*A* and Glu60*B* and the corresponding Lys177*B* and Glu60*A*.

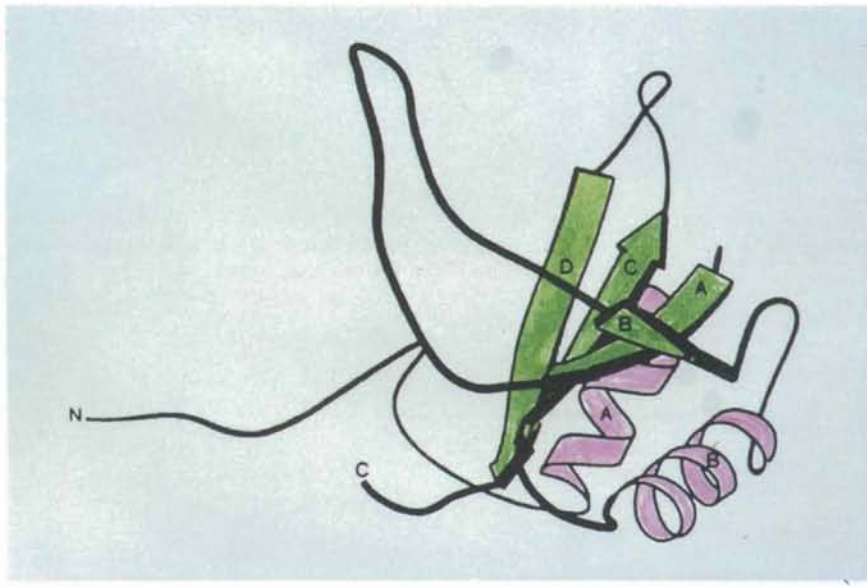

Fig. 6. Schematic diagram of the small subunit of Rubisco (adapted from Knight *et al.*, 1990).

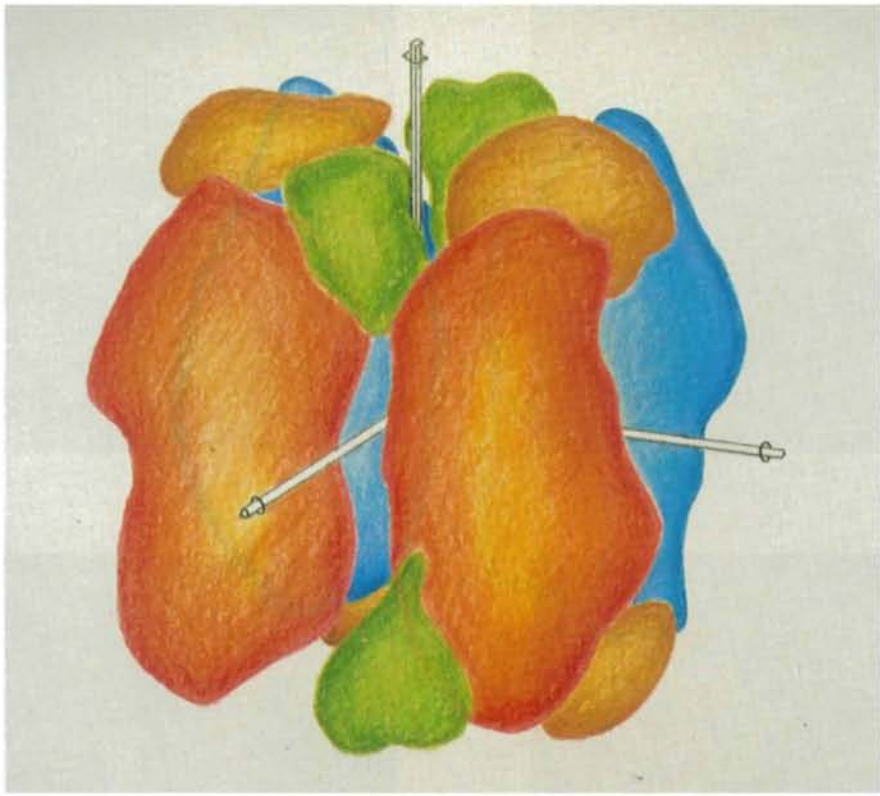

Fig. 7. L_8S_8 Rubisco. The two brick-red L_2 dimers are in front of the two blue L_2 dimers. The eight small subunits are mustard yellow and green.

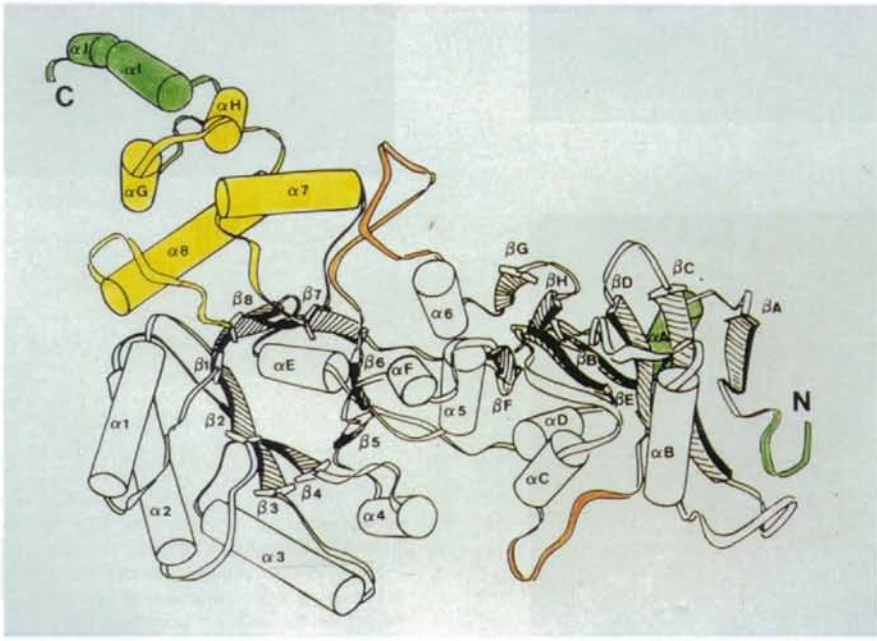

Fig. 8. Schematic diagram of a Rubisco L subunit. Areas where the structures differ between the higher plant L_8S_8 Rubisco and the bacterial L_2 Rubisco are highlighted by different colors. Yellow indicates differences due to the presence of small subunits in L_8S_8, orange areas indicate differences due to different states of the enzyme and green areas represent species differences in the protein chains (adapted from Schneider, Lindqvist *et al.*, 1990).

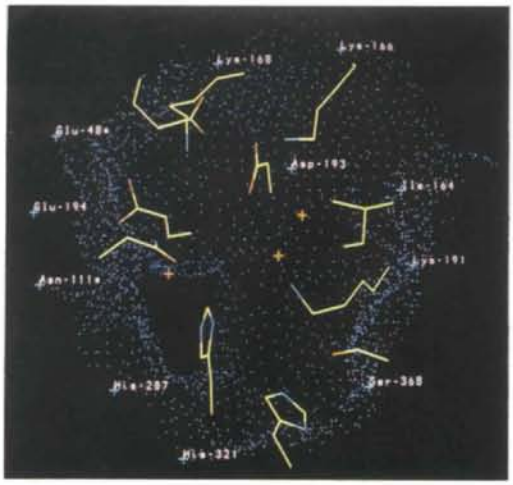

(*a*)

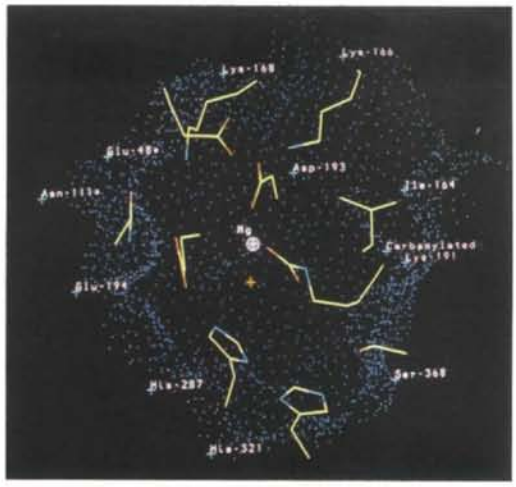

(*d*)

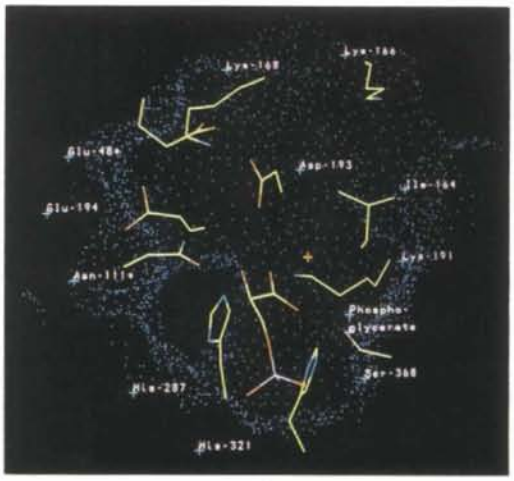

(*b*)

(*e*)

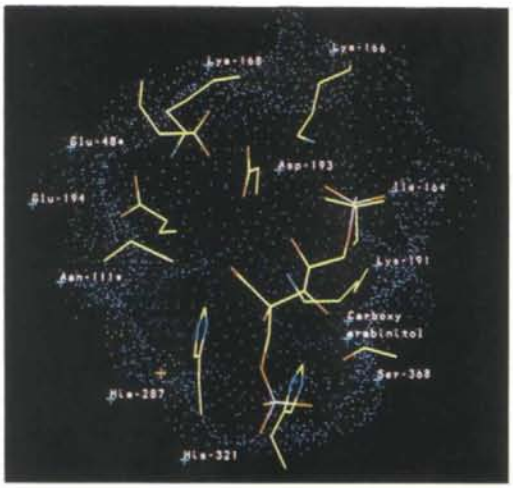

(*c*)

Fig. 10. The active site of Rubisco in different states of activity all shown in the same orientation. The blue dots in the background illustrate the surface of the protein at the active site, not including the side chains shown. The numbers in (*a*) to (*d*) refer to the *Rh. rubrum* Rubisco sequence which is different from the numbering in the spinach sequence in (*e*). (*a*) Non-activated *Rh. rubrum* Rubisco. (*b*) Phosphoglycerate bound to non-activated *Rh. rubrum* Rubisco. (*c*) CABP bound to non-activated *Rh. rubrum* Rubisco. (*d*) Activated *Rh. rubrum* Rubisco. (*e*) CABP bound to activated spinach Rubisco.

of the N-terminal domain are close to or part of the active site. The highly conserved peptide Glu60–Thr65 and the loop 122–127, containing the conserved Asn123, make contacts with residues at the active site.

The active site of Rubisco is thus formed from two different domains, one from each subunit. This arrangement makes the dimer of the large subunit the minimal functional unit: at least two subunits are required to form one active site. Owing to the two-fold symmetry, this automatically generates two active sites per dimer, approximately 30 Å away from each other. Such an arrangement of the active sites in Rubisco, as observed in the crystal structure, has also been invoked from the elegant studies on double mutants, carried out by Hartman and coworkers (Larimer, Lee, Mural, Soper & Hartman, 1987).

The S subunit

The 123 residues of the small subunit are arranged in a four-stranded antiparallel β sheet of topology $(+1, -2x, -1)$, covered on one side by two α helices (Fig. 6). The amino-terminal residues form an arm of irregular structure which extends to a neighboring small subunit and forms the interaction area between the small subunits in the S_4 clusters. The first two β strands are joined by a long loop, which protrudes into the central solvent channel in the L_8S_8 molecule. This loop is wedged between two L subunits and forms extensive interactions with these, despite the fact that part of this loop is absent in Rubisco from cyanobacteria (Nierzwicki-Bauer, Curtis & Haselkorn, 1984). Following the loop there is a β-α-β motif where the two β strands are separated by one strand within the β sheet. The two α helices pack against the antiparallel β sheet forming a hydrophobic core comprising about ten side chains. These residues are all invariant or conservatively substituted in all known sequences of the Rubisco small subunit.

During the structure determination a number of deviations from the published amino-acid sequence (Martin, 1979) of the small subunit became evident. These deviations were detected from the electron density, and in the two instances where they involved cysteine residues they could also be inferred from the positions of bound mercury atoms in the heavy-atom derivatives. It was also apparent (Knight *et al.*, 1990) that the published fold of the tobacco small subunit (Chapman *et al.*, 1988) was incorrect. The tobacco Rubisco structure has now been corrected, using spinach coordinates, refined to high resolution (Curmi, Schreuder, Cascio, Sweet & Eisenberg, 1991) and shown to be very similar to the structure of the spinach enzyme.

The L_8S_8 molecule

The L_8S_8 molecule is shaped like a cube with rounded edges and a side of approximately 110 Å (Fig. 7). The molecular fourfold axis relates four L_2 dimers into a core of eight large subunits $(L_2)_4$. The small subunits are arranged into two separate clusters of four subunits each, $(S_4)_2$, which interact tightly with the large subunits. Each small subunit binds in a deep crevice formed between the tips of two adjacent elongated L_2 dimers at each end of the L_8S_8 molecule. Four faces of the cube-shaped molecule are thus formed by pairs of adjacent L_2 dimers, whereas the remaining two faces are formed by the S_4 clusters. In the centre of the molecule along the local fourfold axis and between the four L_2 dimers, there is a solvent channel extending throughout the molecule.

The interaction areas between the large and the small subunits are quite extensive in spinach L_8S_8 Rubisco, and they involve several regions of amino-acid sequences which are conserved in all S subunits. Some of these regions have been probed by Fitchen, Knight, Andersson, Brändén & McIntosh (1990) by constructing mutants in the S subunit of *Anabena* that do not assemble with the L subunit to functional L_8S_8 molecules in an *E. coli* coexpression system. Two of these mutations affect residues directly involved in L–S interactions. Glu13, which was changed to Val is part of an intricate network of ion-pair interactions involving three additional negatively charged and four positively charged residues from the L subunit. Removal of the negative charge of Glu13 would lead to an unbalanced positive charge being buried in the L–S interface in the case of assembly. The second mutated residue, Pro73, is part of a hydrophobic interaction area comprising Leu74 and Trp70 from the L subunit and Pro73, Phe75 and Pre106 from the small subunit. By changing Pro73 to His, a polar side chain would be buried in this hydrophobic interaction area and it is thus not surprising that this mutant does not form a stable holoenzyme.

Changing the quaternary structure

The amino-acid sequences of the L subunits from spinach and *Rh. rubrum* exhibit 28% identity, and are therefore clearly homologous. As expected, they also have very similar three-dimensional structures. The main differences (Fig. 8) are found in the last 25 residues, which form a C-terminal helical extension to the β/α barrel domain. In the *Rh. rubrum* structure these residues form four α helices, whereas in the spinach large subunit they form only two α helices. In addition, a number of loop regions between secondary-structure elements are different both in lengths and structure.

In order to examine the catalytic role of the C-terminal residues Ranty, Lundqvist, Schneider, Madden, Howard & Lorimer (1990) made a number of deletion mutants at the C-terminus of the *Rh. rubrum* enzyme. Surprisingly it was found that by deleting the last 26 residues, the molecule changed its quaternary structure from dimeric to an octameric L_8 molecule. It was tempting to speculate that an octameric structure had been formed that was similar to the L_8 core of higher plant Rubisco. However, the interactions between the L_2 dimers in the L_8 core of spinach Rubisco occur mainly in the central regions of the elongated L_2 dimers, whereas the C-termini of the L chains are at the ends of the molecule. Furthermore these interactions mainly involve charged side chains in the spinach enzyme, which are different in the *Rh. rubrum* enzyme. It was therefore considered highly unlikely that deletions in the C-terminal regions of the *Rh. rubrum* molecule could induce formation of a quaternary structure similar to that in spinach. Model building showed instead that the deletion exposed two hydrophobic patches on the surface of the L_2 molecule one at each end. A plausible L_8 model could be built in which these hydrophobic patches formed the interaction areas between the dimers. Four such dimers could form an L_8 structure, where the dimers are arranged like a layer of logs in a log cabin (Fig. 9). Such an arrangement would create a larger hole in the middle of the *Rh. rubrum* L_8 molecule than that of the L_8 core of the L_8S_8 molecule. Electron micrographs confirmed this to be the case. In addition it was predicted that a single point mutation of one of the exposed hydrophobic residues in the deletion mutant would restore the L_2 quaternary structure by making the hydrophobic patch more polar. This prediction was confirmed by changing Leu424 to Asn in the deletion mutant.

The moral of these experiments is that changes in quaternary structure can easily result from rather small random mutations and need not necessarily have any physiological relevance. Thus it is not surprising that similar enzymes so frequently have different quaternary structures in different species.

The active site

Structural information on Rubisco from different sources in the activated and non-activated form, without or with bound inhibitors or products is accumulating (Table 2). These crystallographic studies provide information from different stages of the catalytic events and thus allow us to draw some mechanistic conclusions regarding the function of certain conserved residues at the active site as well as conformational changes of the enzyme.

Activation

Activation consists of reaction of a CO_2 molecule with the ε-amino group of Lys201 (191 in *Rh. rubrum* sequence). Subsequent binding of Mg^{II} results in

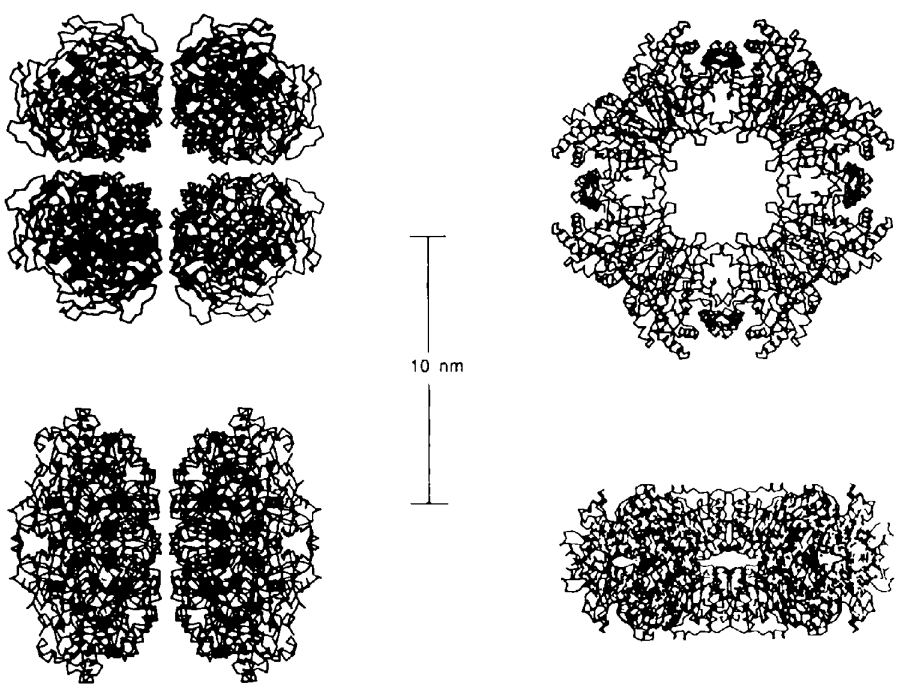

Fig. 9. (*a*) L_8 core of spinach Rubisco as observed in the crystal structure of L_8S_8. (*b*) L_8 mutant of Rubisco from *Rh. rubrum* as deduced from model building.

formation of the active ternary complex. In essence, the activation process changes a positive charge, located at a central position in the active site to a negative charge, resulting in a dramatic change of the microenvironment at the active site. This process influences the electric potential and causes pK_a shifts for certain groups at the active site. Details of the interactions of the metal ion with the enzyme have been studied in the ternary complex of L_2 Rubisco from *Rh. rubrum* with CO_2 and Mg^{II} (Fig. 10*d*) (Lundqvist & Schneider, 1991) and the quaternary complex of the spinach enzyme–CO_2–Mg^{II}–CABP (Fig. 10*e*) (Andersson *et al.*, 1989; Knight *et al.*, 1990).

The amino-acid residue of central importance for activation is Lys201/191. This residue is the last residue in β strand 2 of the β/α barrel and is located at the bottom of the active site. In the non-activated form of the enzyme, the side chain of Lys201/191 forms hydrogen bonds to the main-chain oxygen atom of residue 202/192 and a water molecule. The side chains of residues Asp203/193, His294/194 and Ile173/164 are within van der Waals distance of the Lys side chain (Fig. 10*a*). Upon activation, the side chain of Lys201/191 is carbamylated. One of the carbamate oxygen atoms is ligated to the Mg^{II} ion. Other protein ligands to the metal ion, both in the ternary and quaternary complex of Rubisco, are the side chains of Asp203/193 and Glu204/194 (Figs. 10*d*, 10*e*) (Andersson *et al.*, 1989; Lundqvist & Schneider, 1991). In the activated ternary complex of Rubisco from *Rh. rubrum*, at least one water molecule has been identified in the first coordination sphere of the metal ion.

Site-directed mutagenesis experiments have been performed to probe the function of certain residues involved in activation and metal binding. Lys201/191 was changed to Glu in an attempt to make a permanently activated Rubisco (Estelle, Hanks, McIntosh & Somerville, 1985). The mutant was, however, catalytically inactive. Model building experiments based upon the crystal structures of activated Rubisco suggest that the glutamic acid side chain is too short to participate in the formation of the metal-binding site. All mutations at Asp203/193 and Glu204/194 destroy the overall activity of the enzyme and demonstrate the strict requirement of an intact metal-binding site for catalysis (Lorimer, Gutteridge & Madden, 1987).

An interesting observation was made concerning the structure of the binary complex of non-activated Rubisco with the product, PGA (Lundqvist & Schneider, 1989*a*). In this complex, the carboxyl group of phosphoglycerate interacts with the side chain of Lys201/191 (Fig. 10*b*). After activation, this side chain is negatively charged and participates in the binding of a metal ion (Fig. 10*d*). Here, we observe a clear example that the simple replacement of a charge changes the character of a binding site completely: from an anion binding site to a metal-ion binding site in disagreement with theoretical studies (Hwang & Warshel, 1988). On behalf of nature's protein engineering through evolution, we have claimed the Alliant Inc. award (Hwang & Warshel, 1988) that will be given "to the first person who succeeds in an effective polarity reversal".

One function of the metal ion has been suggested (Lundqvist & Schneider, 1989*b*) from a comparison of inhibitor binding to activated and non-activated forms of the enzyme. The substrate, RuBP, can bind to the active site in two basically different ways: the phosphate groups at their proper binding sites or with the phosphate groups interchanged. Crystallographic analysis of the binding of the inhibitor CABP to non-activated Rubisco from *Rh. rubrum* (Fig. 10*c*) and activated spinach Rubisco (Fig. 10*e*) (Andersson *et al.*, 1989; Knight *et al.*, 1990) revealed a different binding of the inhibitor in the two species. In the absence of the metal ion, the inhibitor is bound 'the other way around' at the active site. This finding thus suggests that the metal ion is at least partly responsible for proper orientation of the substrate at the active site.

The decisive factor that differentiates the binding modes of CABP in these two complexes is the environment of the carboxyl group of CABP. This group is in the central region of the barrel in both complexes. These regions are quite different in the activated and deactivated forms. Activation brings an Mg^{II} ion into this central region of the active site, poised to bind the substrate carboxyl group.

Binding of phosphorylated compounds to non-activated Rubisco

Binding of the product, PGA, to the non-activated enzyme has been studied in order to localize the active site and identify one of the phosphate-binding sites (Fig. 10*b*) (Lundqvist & Schneider, 1989*a*). The phosphate group binds to residues located at loops 5 and 6 of the β/α barrel which provide two positively charged side chains, Arg295 (not shown in Fig. 10) and His327/321. The carboxyl group of PGA interacts with Lys201/191, the site of activation. In the non-activated enzyme, CABP binds across the funnel-shaped active site with one of the phosphate groups bound to the same site as utilized for the binding of PGA, close to loops 5 and 6 (Fig. 10*c*). The second phosphate group is bound at the opposite end of the funnel and interacts with the side chain of Lys175/166 in loop 1, a conserved residue at the active site. The negatively charged 2-carboxyl group of the analogue is close to the side chain of Lys201/191. This phosphate group also interacts

with the main-chain nitrogen atoms from Gly403 at the N-terminal end of a very short helix in loop 8. The helix dipole compensates part of the negative charge of the phosphate (Hol, 1985).

Binding of a reaction-intermediate analogue, CABP, to activated Rubisco

The reaction intermediate 3-keto-CABP formed on the enzyme after CO_2 addition, is not sufficiently stable for a structure determination of its complex with Rubisco, even though it can be isolated and used as a probe for the catalytic efficiency of mutant Rubisco molecules (Pierce *et al.*, 1986).

In order to infer the mode of binding of the six-carbon reaction intermediate and groups on the enzyme that are involved in these bonds, we have studied the Rubisco complex with the reaction-intermediate analogue, CABP. This analogue forms an extremely stable complex with activated spinach enzyme which has a half-life of about one year, and which can be regarded as simulating one of the transition states of the catalytic reaction.

The CABP complex with activated Rubisco has been studied by cocrystallization with spinach Rubisco, activated in solution. CABP binds in an extended conformation across the barrel (Fig. 10*e*), anchored to the protein by the two phosphate-binding sites at opposite ends of the funnel-shaped active site as described above.

The carboxyl group of CABP binds to Mg^{II} through one of its oxygen atoms. In addition, the two lysine residues of loop 1, Lys175 and Lys177, as well as a third lysine residue, Lys334 from the flexible loop number 6 of the barrel, are within interaction distance of the carboxyl group. Two hydroxyl groups of CABP are ligated to the magnesium ion on one side of CABP. The third hydroxyl group forms a hydrogen bond on the other side to the hydroxyl group of an invariant serine residue, Ser379, in loop 7.

A possible role for the small subunit

Once the enzyme has fixed the gaseous substrate, oxygen or carbon dioxide, and added it to RuBP, the reaction is committed to either oxygenation or carboxylation. Any attempt to change the carboxylation/oxygenation ratio by mutagenesis must therefore concentrate on reactions up to and including this step. The most obvious choice is to try to modify those interactions that stabilize the transition states for addition of these gaseous substrates. Unfortunately we know next to nothing about these factors for oxygen as a substrate. The complex between activated Rubisco and CABP can, however, to a first approximation be regarded as a transition-state analogue for the addition of CO_2, even though it is an analogue to the reaction intermediate, 3-keto-CABP. What can be inferred about these factors that could aid such mutagenesis experiments from the structural knowledge at hand? Two aspects of this question will be discussed here; the effect of the small subunits and the conformational differences between the activated and nonactivated forms of the enzyme.

Residues from the small subunit do not interact directly with the active sites in the L_8S_8 molecule. Nevertheless, the catalytic activity of the enzyme is modified by the small subunit since removal of these subunits from the L_8 core decreases carboxylation activity by two orders of magnitude (Andrews, 1988). We have therefore compared an L_2 dimer from the L_8S_8 molecule of spinach Rubisco with the L_2 dimer of the complete *Rh. rubrum* Rubisco molecule (Schneider, Knight *et al.*, 1990). We found that the overall structures of these dimers are remarkably similar. The domain structures are similar and they are arranged in essentially the same way in the subunits which in turn form similar dimers. The differences that occur are mainly of three types (Fig. 8).

The first type involves the N- and C-terminal residues. These differences reflect in all probability species difference and will not be described here, although they might be of catalytic interest since some of these residues are close to the active site in the spinach enzyme. The second type involves two loop regions, residues 60–80 and 331–342, which are disordered in the nonactivated enzyme but ordered in the activated form where they contribute important catalytic groups. These will be discussed later. The third type is more subtle and can be associated with indirect effects by the small subunit on the active site.

This difference was discovered when we compared the β/α barrel structures of the C-terminal domains. All eight β strands, six of the α helices and most of the loop regions of the barrel structures superimposed very well. However, the remaining two helices $\alpha 7$ and $\alpha 8$ and the two loop regions that connect them with the β strands in the active-site region are significantly different although the actual conformations of the loop regions are quite similar (shown in yellow in Fig. 8). These two loop regions are both part of the active site of the enzyme. Loop 7 contains the strictly conserved Ser379, which is involved in the binding of both CABP and product. Loop 8 is part of one of the phosphate-binding sites. A difference in these parts of the active site will result in differences in substrate binding and hence in catalytic rates. Is this difference due to the presence of small subunits in the spinach enzyme?

The answer is quite clear. If the *Rh. rubrum* L_2 dimer is used to model an L_8S_8 molecule similar to spinach Rubisco there will be steric collisions

between the small subunits and helix $\alpha 8$ as well as parts of loop 8 of the L_2 dimers. In the spinach enzyme the positions of these regions are sufficiently different so that they form a smooth interaction area with the small subunits. The position of helix $\alpha 7$ is also different to avoid steric interference with helix $\alpha 8$. It is thus apparent that the small subunits influence the position of two crucial loop regions in the active site of Rubisco and thereby modulate the activity of higher plant Rubisco molecules. It will be interesting to see to what extent the catalytic activities of wild-type L_8S_8 Rubisco can be modified by mutations in this subunit interaction area.

Stabilization of the transition state for CO_2 *addition*

One of the oxygen atoms of the carboxyl group of CABP is coordinated to the active-site Mg^{II} ion. The second oxygen atom forms a hydrogen bond to Lys344 which in turn interacts with Glu60 (Fig. 10*e*). There is strong biochemical and genetic evidence that these interactions are of crucial importance for stabilization of the transition states for addition of CO_2 or O_2 and hence for the relative catalytic rates of carboxylation and oxygenation.

Exchange of Mg^{II} for other metal ions produces either catalytically inert Rubisco molecules or an enzyme species with a drastically different carboxylation/oxygenation ratio. This ratio is usually referred to in terms of a specificity factor, τ, which is the ratio of $k_{cat}(V_{max}/K_m)$ for the two activities (Laing, Ogren & Hageman, 1974).

Rubisco mutants where Lys334 is replaced by other residues (Soper, Mural, Larimer, Lee, Machanoff & Hartman, 1988) are catalytically inactive, bind the competitive inhibitor 6-phosphogluconate but do not form strong complexes with CABP. Replacement of Glu60 by the shorter side chain of Asp gives a drastic reduction in catalytic rate by at least three orders of magnitude. What about replacement by a longer side chain? Fred Hartman and his colleagues have addressed this question in a clever way (Smith, Larimer & Hartman, 1990). They replaced the Glu residue by Cys to produce a catalytically inert mutant. Catalytic activity was restored by treating the mutant with iodoacetate. The Cys side chain becomes carboxymethylated and an acidic side chain is produced that contains an extra sulfur atom compared to the Glu side chain. This chemically modified mutant has a fivefold lower specificity factor than the wild-type enzyme. This experiment has produced the first site-directed mutant with a different specificity factor and as such it demonstrates the possibility of changing the carboxylation/oxygenation ratio even though the catalytic rate of the enzyme has decreased by one order of magnitude, and the specificity factor has changed in favour of oxygenation instead of carboxylation.

Lys334 is at the tip of loop 6 which connects β strand 6 to α helix 6 of the β/α barrel (Fig. 11). This loop is flexible. In the activated ternary complex the loop has different conformations in the two crystallographically independent subunits. None of these conformations is similar to that found in the spinach activated quaternary CABP complex where this loop is clamped over the CABP molecule, bringing the positively charged NH_3 group of Lys334 close to the carboxyl group of CABP. It therefore seems possible that CO_2 addition to RuBP is coupled to a conformational transition of this loop so that Lys334 can stabilize the transition state of this partial reaction.

The catalytic properties of temperature-sensitive Rubisco mutants that have been recovered from the unicellular green alga *Chlamydomonas reinhardii* (Chen & Spreitzer, 1989) can be correlated to such a conformational transition. One of these mutants, where Val331 was mutated to Ala, changed the specificity factor from 62 in the wild-type enzyme to 39 in the mutant. A second suppressor mutation, Thr342 to Ile, partly restored this factor to a value of 52.

The corresponding residues in the spinach enzyme, Val331 and Thr342, are close together in a hydrophobic pocket at the base of loop 6. The first mutation, Val331 to Ala, would change the packing of hydrophobic side chains in this pocket and influence the conformational transition and probably also the exact position of Lys334 in the transition state.

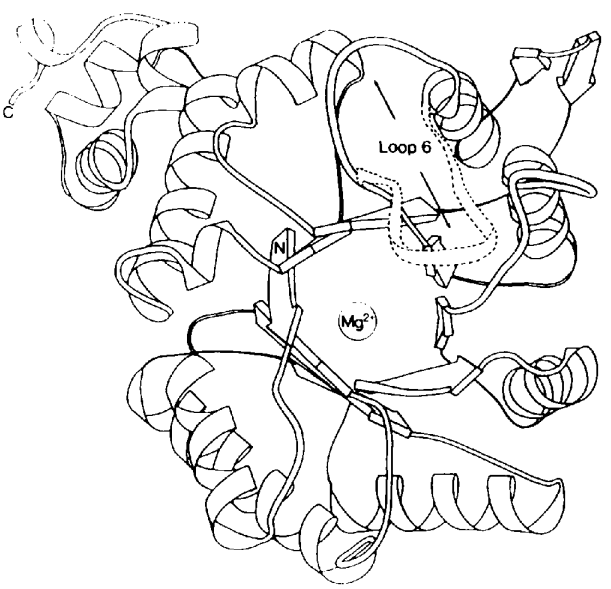

Fig. 11. Schematic drawing of the C-terminal domain of Rubisco illustrating 'open' and 'closed' (dashed line) conformations of loop 6 of the β/α barrel. The position of the metal ion in the active site is indicated. (Courtesy of Tomas Lundqvist.)

The second mutation, Thr342 to Ile, would restore, at least partly, the hydrophobic core and hence the kinetic effects of this loop. Interestingly these two positions are invariant in almost all Rubisco molecules except in *Alcaligenes eutrophus* where almost the same double mutations have occurred naturally; residue 331 is Ala and 342 is Val. It is thus apparent that this loop region is a very interesting target for attempts to obtain a modified Rubisco where the specificity factor has increased compared to that in wild-type enzyme. Such studies are now underway.

*The elusive role of Lys*175

Enolization of the substrate, RuBP is the first step in catalysis, both in the carboxylation and the oxygenation reaction. This step is initiated by abstraction of the proton at the C(3) position of the substrate. This partial reaction can be followed experimentally, *e.g.* by measuring the 'wash-out' of radioactivity from RuBP, labelled with tritium at the C(3) position. Lys175 has been proposed to be the enzymic base which abstracts the proton and initiates catalysis (Hartman *et al.*, 1987, Lorimer & Hartman, 1988). The evidence presented to support such a role seemed convincing: the lysine residue was shown to be at the active site, both by site-directed labelling experiments and from crystallographic studies. The side chain has an unusually low pK_a of approximately 7·9 (Hartman, Milanez & Lee, 1985). This pK_a value agrees well with the value of 7·5 determined from the pH dependency of the deuterium isotope effect for proton abstraction from C(3) of the substrate (Van Dyk & Schloss, 1986). Site-directed mutagenesis experiments further supported this notion. The replacement of Lys175 with Gly yielded an inactive enzyme (Hartman *et al.*, 1987). The mutant was able to undergo activation and did bind the inhibitor CABP, but did not catalyze the enolization reaction (Lorimer & Hartman, 1988). Thus, the case for the role of Lys175 seemed closed: it is the base which abstracts a proton from the C(3) position of the substrate.

However, conflicting evidence comes from crystallographic studies. In the refined structure of the complex of activated spinach Rubisco with the inhibitor CABP the side chain of Lys175 is close to one of the phosphate groups and is not in the vicinity of the C(3) position of the substrate. Furthermore, model-building experiments show that this side chain cannot be brought close to the C(3) carbon atom, given the orientation of the substrate and the conformation of loop 1 as observed in the quaternary complex. Shortening the distance between the Nε of Lys175 to the C(3) atom sufficiently for proton abstraction to occur, would require that either the mode of substrate binding or the course of the main chain of loop 1 would have to change significantly. In all other forms and complexes of the enzyme studied so far by crystallographic methods, the conformation of loop 1 is, however, highly similar to that observed in the quaternary complex.

This discrepancy between the results from biochemical studies and site-directed mutagenesis on one hand and the crystallographic analysis on the other hand is at the moment somewhat unsettling since it might mean that some of the conclusions based on seemingly sound biochemical, crystallographic or genetic data are wrong. At present, this issue is being addressed by a combined effort of protein-crystallographic, biochemical and protein-engineering techniques.

References

ANDERSSON, I. & BRÄNDÉN, C.-I. (1984). *J. Mol. Biol.* **172**, 363–366.

ANDERSSON, I., KNIGHT, S., SCHNEIDER, G., LINDQVIST, Y., LUNDQVIST, T., BRÄNDÉN, C.-I. & LORIMER, G. (1989). *Nature (London)*, **337**, 229–234.

ANDERSSON, I., TJÄDER, A.-C., CEDERGREN-ZEPPEZAUER, E. & BRÄNDÉN, C.-I. (1983). *J. Biol. Chem.* **258**, 14088–14090.

ANDREWS, T. J. (1988). *J. Biol. Chem.* **263**, 12213–12219.

ANDREWS, T. J. & LORIMER, G. H. (1987). *The Biochemistry of Plants*, edited by M. D. HATCH, Vol. 10, pp. 131–218. Orlando: Academic Press.

BAKER, T. S., EISENBERG, D. & EISERLING, F. A. (1977). *Science*, **196**, 293–295.

BAKER, T. S., EISENBERG, D., EISERLING, F. A. & WEISSMAN, L. (1975). *J. Mol. Biol.* **91**, 391–399.

BAKER, T. S., SUH, S. W. & EISENBERG, D. (1977). *Proc. Natl Acad. Sci. USA*, **74**, 1037–1041.

BARCENA, J. A., PICKERSGILL, R. W., ADAMS, M. J., PHILLIPS, D. C. & WHATLEY, F. R. (1983). *EMBO J.* **2**, 2363–2367.

BARRACLOUGH, R. & ELLIS, R. J. (1980). *Biochim. Biophys. Acta*, **608**, 19–31.

BRICOGNE, G. (1976). *Acta Cryst.* A**32**, 832–847.

CALVIN, M. (1956). *J. Chem. Soc.* pp. 1875–1915.

CHAPMAN, M. S., SUH, S. W., CASCIO, D., SMITH, W. W. & EISENBERG, D. (1987). *Nature (London)*, **329**, 354–356.

CHAPMAN, M. S., SUH, S. W., CURMI, P. M. G., CASCIO, D., SMITH, W. W. & EISENBERG, D. (1988). *Science*, **241**, 71–74.

CHEN, X. & SPREITZER, R. J. (1989). *J. Biol. Chem.* **264**, 3051–3053.

CHOE, H.-W., JAKOB, R., HAHN, U. & PAL, G. P. (1985). *J. Mol. Biol.* **185**, 781–783.

CURMI, P. M. G., SCHREUDER, H., CASCIO, D., SWEET, R. & EISENBERG, D. (1991). *J. Biol. Chem.* In the press.

ELLIS, R. J. & VAN DER VEIS, S. M. (1988). *Photosynth. Res.* **16**, 101–115.

ESTELLE, M., HANKS, J., MCINTOSH, L. & SOMERVILLE, C. (1985). *J. Biol. Chem.* **260**, 9523–9526.

FARBER, G. K. & PETSKO, G. A. (1990). *Trends Biochem. Sci.* **15**, 228–234.

FITCHEN, J. H., KNIGHT, S., ANDERSSON, I., BRÄNDÉN, C.-I. & MCINTOSH, L. (1990). *Proc. Natl Acad. Sci. USA*, **87**, 5768–5772.

GATENBY, A. A., VAN DER VIES, S. M. & ROTHSTEIN, S. J. (1987). *Eur. J. Biochem.* **168**, 227–231.

HARTMAN, F. C., MILANEZ, S. & LEE, E. H. (1985). *J. Biol. Chem.* **260**, 13968–13975.

HARTMAN, F. C., SOPER, T. S., NIYOGI, S. K., MURAL, R. J., FOOTE, R. S., MITRA, S., LEE, E. H., MACHANOFF, R. & LARIMER, W. F. (1987). *J. Biol. Chem.* **262**, 3496–3501.
HOL, W. G. H. (1985). *Prog. Biophys. Mol. Biol.* **45**, 149–195.
HWANG, J. K. & WARSHEL, A. (1988). *Nature (London)*, **334**, 270–272.
JANSON, C. A., SMITH, W. W., EISENBERG, D. & HARTMAN, F. C. (1984). *J. Biol. Chem.* **259**, 11594–11596.
KETTLEBOROUGH, C. A., PERRY, M. A., BURTON, S., GUTTERIDGE, S., KEYS, A. J. & PHILIPS, A. L. (1987). *Eur. J. Biochem.* **107**, 335–342.
KNIGHT, S., ANDERSSON, I. & BRÄNDÉN, C.-I. (1989). *Science*, **244**, 702–705.
KNIGHT, S., ANDERSSON, I. & BRÄNDÉN, C.-I. (1990). *J. Mol. Biol.* **215**, 113–160.
LAING, W. A., OGREN, W. L. & HAGEMAN, R. H. (1974). *Plant Physiol.* **54**, 678–685.
LARIMER, F. W., LEE, E. H., MURAL, R. J., SOPER, T. S. & HARTMAN, F. C. (1987). *J. Biol. Chem.* **262**, 15327–15329.
LORIMER, G. (1981). *Biochemistry*, **20**, 1236–1240.
LORIMER, G., GUTTERIDGE, S. & MADDEN, M. W. (1987). *Plant Molecular Biology*, edited by D. VON WETTSTEIN & N.-H. CHUA, pp. 21–31. New York: Plenum Press.
LORIMER, G. & HARTMAN, F. C. (1988). *J. Biol. Chem.* **263**, 6468–6471.
LORIMER, G. & MIZIORKO, H. M. (1980). *Biochemistry*, **19**, 5321–5328.
LUNDQVIST, T. & SCHNEIDER, G. (1989*a*). *J. Biol. Chem.* **264**, 3643–3646.
LUNDQVIST, T. & SCHNEIDER, G. (1989*b*). *J. Biol. Chem.* **264**, 7078–7083.
LUNDQVIST, T. & SCHNEIDER, G. (1991). *Biochemistry*, **30**, 904–908.
MARTIN, P. G. (1979). *Aust. J. Plant. Physiol.* **6**, 401–408.
MIZIORKO, H. M. & LORIMER, G. (1983). *Annu. Rev. Biochem.* **52**, 507–535.
NAKAGAWA, H., SUGIMOTO, M., KAI, Y., HARADA, S., MIKI, K., KASAI, N., SAEKI, K., KAKUNO, T. & HORIO, T. (1986). *J. Mol. Biol.* **191**, 577–578.
NEWMAN, J. & GUTTERIDGE, S. (1990). *J. Biol. Chem.* **265**, 15154–15159.
NIERZWICKI-BAUER, S. A., CURTIS, S. E. & HASELKORN, R. (1984). *Proc. Natl Acad. Sci. USA*, **81**, 5961–5965.
PAL, G. P., JAKOB, R., HAHN, U., BOWIEN, B. & SAENGER, W. (1985). *J. Biol. Chem.* **260**, 10768–10770.
PIERCE, J. & GUTTERIDGE, S. (1985). *Appl. Environ. Microbiol.* **49**, 1094–1100.
PIERCE, J., LORIMER, G. & REDDY, G. S. (1986). *Biochemistry*, **19**, 1636–1644.
RANTY, B., LUNDQVIST, T., SCHNEIDER, G., MADDEN, M., HOWARD, R. & LORIMER, G. (1990). *EMBO J.* **9**, 1365–1375.
SCHNEIDER, G., BRÄNDÉN, C.-I. & LORIMER, G. (1984). *J. Mol. Biol.* **175**, 99–102.
SCHNEIDER, G., BRÄNDÉN, C.-I. & LORIMER, G. (1986). *J. Mol. Biol.* **187**, 141–143.
SCHNEIDER, G., KNIGHT, S., ANDERSSON, I., LINDQVIST, Y., LUNDQVIST, T. & BRÄNDÉN, C.-I. (1990). *EMBO J.* **9**, 2045–2050.
SCHNEIDER, G., LINDQVIST, Y., BRÄNDÉN, C.-I. & LORIMER, G. (1986). *EMBO J.* **5**, 3409–3415.
SCHNEIDER, G., LINDQVIST, Y. & LUNDQVIST, T. (1990). *J. Mol. Biol.* **211**, 989–1008.
SMITH, H. B., LARIMER, F. W. & HARTMAN, F. C. (1990). *J. Biol. Chem.* **265**, 1243–1245.
SOMERVILLE, R. C. & SOMERVILLE, S. C. (1984). *Mol. Gen. Genet.* **193**, 214–219.
SOPER, T. S., LARIMER, F. W., MURAL, R. J., LEE, E. H. & HARTMAN, F. C. (1989). *J. Protein Chem.* **8**, 239–249.
SOPER, T. S., MURAL, R. J., LARIMER, F. W., LEE, E. H., MACHANOFF, R. & HARTMAN, F. C. (1988). *Protein Eng.* **2**, 39–44.
SUH, S. W., CASCIO, D., CHAPMAN, M. S. & EISENBERG, D. (1987). *J. Mol. Biol.* **197**, 363–365.
TABITA, F. R. & MCFADDEN, B. A. (1974). *J. Biol. Chem.* **249**, 3459–3464.
VAN DYK, D. & SCHLOSS, J. V. (1986). *Biochemistry*, **25**, 5145–5156.

Acta Cryst. (1991). B**47**, 835–843

Ordering and Structural Vacancies in Non-Stoichiometric Cu–Al γ Brasses

BY E. H. KISI

Division of Science and Technology, Griffith University, Nathan, Queensland 4111, *Australia*

AND J. D. BROWNE

Department of Mechanical Engineering, University of Newcastle, NSW 2308, *Australia*

(*Received* 13 *February* 1991; *accepted* 9 *May* 1991)

Abstract

γ-Brass structures are based on the cubic packing of 26-atom clusters which have, as concentric subunits, an inner and an outer tetrahedron (IT, OT), an octahedron (OH) and a cuboctahedron (CO). Cu_9Al_4 [$M_r = 679{\cdot}37$, $P\bar{4}3m$, $a = 8{\cdot}7046$ (1) Å, $V = 659{\cdot}5$ Å^3, $Z = 4$, $D_x = 6{\cdot}846$ Mg m^{-3}, $R_{wp} = 0{\cdot}051$, $R_B = 0{\cdot}017$ for 238 powder reflections] is the stoichiometric γ brass of the Cu–Al system and contains two clusters (A, B) per unit cell. Al atoms occupy a 4(e) (IT) site in cluster A and a 12(i) (CO) site in cluster B. Cu atoms occupy the remaining 4(e) (OT), 6(f) (OH) and 12(i) (CO) sites of cluster A and the two 4(e) (IT, OT) and a 6(g) (OH) site of cluster B. The structure has considerable solubility for Al and this

0108-7681/91/060835-09$03.00